

# Zero-sound in nuclear matter with the asymmetry parameter $-1 \leq \beta \leq 1$

V.A. Sadovnikova (NRC "Kurchatov Institute", St. Petersburg, INP)

November 25, 2019

## Abstract

Results for the frequencies of zero-sound excitations in the isospin asymmetric nuclear matter are presented for the different parameters of asymmetry  $-1 \leq \beta \leq 1$ . The dispersion equations are constructed within the random phase approximation. We use the effective Landau-Migdal quasiparticle interaction with the special isospin dependence of the phase volume in the normalization factor  $C_0$ . In the paper we present zero-sound branches of the dispersion equation solutions in the symmetric, asymmetric and neutron matter. The branches correspond to the different channels of decay of the zero-sound excitation in the nuclear matter or nuclei. In the asymmetric nuclear matter we obtain three branches of solutions on the physical and unphysical sheets of the complex frequency plane,  $\omega_{s\tau}(k, \beta)$ ,  $\tau = p, n, np$ . We demonstrate the change of branches with  $\beta$  and conversion of the three branches into two branches in symmetric nuclear matter ( $\beta = 0$ ) and into one branch in the neutron matter ( $\beta = 1$ ).

## 1 Introduction

At the present time a lot of attention is paid to the study of the nuclear matter properties at the different densities, asymmetry parameters, temperature, types of interactions, the particle composition. Our main results presented in this paper are the branches of zero-sound excitations in the asymmetric nuclear matter. There are a lot of publications describing the different types of the excited collective states and their decays. In paper [1] the three types of excited states are obtained in the framework of local isospin density approximation approach based on the density energy functional, their contribution to the energy-weighted sum rules in nuclei are evaluated.

In the papers [2, 3] the energies and damping rate of the giant excitations and the corresponding strength functions are considered in the asymmetric nuclear matter and in nuclei at

different temperature. The zero-sound dispersion equation was constructed on the basis of the non-Markovian kinetic equation. Two (isoscalar and isovector) complex modes are obtained and a new mode predicted which exist in ANM only.

In [4] propagation of the sound modes is considered on the basis of the kinetic theory including collisions, temperature and memory effects. In [5] results for zero sound in nuclear matter obtained in the framework of Landau-Migdal theory, are applied to the giant resonances in nuclei. To calculate the width of resonances and its temperature dependence the developed kinetic theory was used. The role of the effective nucleon-nucleon interaction in description of the giant resonances in the hot nuclei and dependence of the energies and widths on the temperature are investigated in [6]. In [7] a linear response theory starting from a relativistic kinetic equations is developed within a Quantum-Hadrodynamics effective field picture of the hadronic phase of nuclear matter. The dispersion relations are derived, they give the sound phase velocity and the internal structure of the normal collective modes, stable and unstable.

In our paper we investigate zero-sound excitations in the normal cold Fermi-liquid, consisting from the neutrons and protons at the different values of the asymmetry parameter. We study how the branches of solutions change with  $\beta$ . The dispersion equation for the collective excitations in the Fermi liquid theory [8, 9] is considered. In this equation we pay a special attention to the analytical structure of the polarization operators which contain the logarithmic functions. The cuts related to the logarithms are formed by the free particle-hole  $ph$  pairs. The stable collective solutions are placed on the right of cuts on the complex frequency plane at small wave vectors  $k$ . When  $k$  increase, there is an overlapping of collective and  $ph$  modes. At these  $k$  we look for solutions under the logarithmic cuts on the nearest unphysical sheet and obtain a complex solutions placed on the unphysical sheet. The imaginary part of solutions is interpreted as a width of excitation appeared due to admixture of the free  $ph$  pairs to the collective modes.

Our approach was tested in the symmetric nuclear matter (SNM) where the branches of the nucleon zero-sound, isobar zero-sound and pion excitations were calculated [10, 11].

An isospin asymmetric nuclear matter is characterized by the density of the neutrons  $\rho_n$  and protons  $\rho_p$ . An asymmetry parameter is defined as

$$\beta = (\rho_n - \rho_p)/(\rho_n + \rho_p). \quad (1)$$

The Fermi-momentum for the protons and neutrons are

$$p_{Fn} = \left( \frac{3\pi^2}{2} (1 + \beta) \rho \right)^{1/3}, \quad p_{Fp} = \left( \frac{3\pi^2}{2} (1 - \beta) \rho \right)^{1/3}, \quad p_0 = \left( \frac{3\pi^2}{2} \rho_0 \right)^{1/3}, \quad (2)$$

where  $\rho_0 = 0.17 \text{ fm}^{-3}$ . We consider the isovector external field  $V_0^\tau(\omega, k) = E_0 \sum_i (\tau_z)_i e^{i\vec{r}_i \cdot \vec{k}} e^{-i(\omega + i\eta)t}$  which generates the system of the effective fields  $V_{eff}^{\tau_1 \tau_2}(\omega, k)$ . The system is similar to the one

obtained for the isovector dipole external field in [8]. We investigate the solutions of the dispersion equation of this system. The frequencies and widths of the solutions in ANM are studied as the functions of the momentum  $k$  and symmetry parameter  $\beta$  at density  $\rho = \rho_0$ , and the effective Landau-Migdal quasiparticle interaction.

The effective fields  $V_{eff}^{\tau_1\tau_2}(\omega, k)$  describe the two types of excitations, generated in the system by the external field: noninteracting (free) particle-hole pairs ( $ph$ -mode)  $\omega_{ph}^\tau(k)$  and the zero sound collective mode  $\omega_s(k)$ .

In SNM at small  $k$ , the collective solutions  $\omega_s(k)$  are real, but with  $k$  increasing there is an overlapping of the collective and  $ph$ -modes. We obtain the complex solution in the region of overlapping using the analytical structure of polarization operator. The imaginary part  $\text{Im}\omega_s(k)$  characterizes the width of the collective mode which appeared due to mixture with the free  $ph$  pairs. In SNM the isospin of these pairs is not fixed. The analogous process in the nuclei following by the nucleon escape, is characterized by the escape width.

In SNM, besides  $\omega_s(k)$ , we obtain one more branch of the collective solutions (we denote it  $\omega_{s1}(k)$ ). It is placed on the unphysical sheet and starts at some  $k = k_c$ . The feature of this branch is its decay on the  $ph$  pairs of the one isospin. It may be the proton or the neutron  $ph$  pairs, but not the mixture. This branch is an important element linking the solutions in SNM and in ANM.

In ANM we consider three possible mechanisms of damping of the collective excitations, three decay channels. We consider separately the overlapping of the collective mode with 1) the free neutron  $ph$ -pairs, 2) the free proton  $ph$ -pairs and 3) with the nucleon pairs whose isospin is not adjusted. We obtain three different branches of solutions:  $\omega_{sn}(k, \beta)$  in the case (1);  $\omega_{sp}(k, \beta)$  when the overlapping with the proton  $ph$ -pairs is considered (case 2) and  $\omega_{snp}(k, \beta)$  in the case (3). These branches are calculated on the different unphysical sheets (Sect.3) <sup>1</sup>.

When we investigate the zero sound dispersion equations we can obtain several branches of the collective solutions. The question appears: which of the branches can be compared with the real physical excitations, stable or unstable? We consider as the physical sheet of the complex  $\omega$ -plane that one where the real collective solutions and the energies of the free  $ph$ -pairs are placed on the real axis. These solutions describe the free  $ph$  mode and the stable collective modes in the matter and we name them 'the physical solutions'. The solutions at the other parameters (the other  $k$ , the densities, the asymmetry parameters, and so on) we consider as physical ones if it is possible to do the analytical continuation over the necessary parameter from the stable solutions to the point of the interest [12]. The analytical continuation can be made to the physical or unphysical sheets. This permits us to know the nature of the every branch and control how they behave with change of  $k$  and  $\beta$ . When we consider the physical functions in nuclei, for example, the strength

---

<sup>1</sup>In ANM the branches  $\omega_{si}(k, \beta)$ ,  $i = n, p, np$  depend on  $k$  and  $\beta$  but when it is not important we omit  $\beta$ :  $\omega_{si}(k)$ .

functions of the excitations in nucleus  $A$ , we take into account all physical solutions obtained at the given  $k_A$  and  $\beta_A$ . The wave vector  $k_A$  can be found for the given  $A$  and the kind of excitation using the Steinwedel-Jensen model [13], as a sample.

It is important to note (Sect.3) that at  $\beta > 0$  the stable solutions belong to the branches  $\omega_{sn}(k, \beta)$ , at  $\beta = 0$  – to  $\omega_s(k)$  and at  $\beta < 0$  – to  $\omega_{sp}(k, \beta)$ . It means that at  $\beta > 0$  the stable solutions begin to damp with  $k$  increasing due to the mixture with the neutron free pairs  $\omega_{ph}^n(k)$ , at  $\beta < 0$  due to mixture with  $\omega_{ph}^p(k)$  and at  $\beta = 0$  the mixture with the both the proton and neutron pairs. Technically it is expressed in that at  $\beta > 0$  the real solutions go with  $k$  increasing under the logarithmic cut of the neutron polarization operator and we name them  $\omega_{sn}(k)$ . At  $\beta < 0$  the real solutions go under the logarithmic cut of proton polarization operator. This is the branch  $\omega_{sp}(k)$ . At  $\beta = 0$  the real solutions go under the logarithmic cut of the both proton and neutron polarization operators. This is the branch  $\omega_s(k)$ .

In our investigation there are four special values of the wave vector:  $k^p, k_t, k^{np}, k_c$ . At small  $\beta$  we have  $k^p < k_t < k^{np} < k_c$ . The character of branches and transitions to SNM and the neutron nuclear matter (NNM) depend of the interval where  $k$  is considered. The wave vectors  $k_t, k^p, k^{np}$  are functions on  $\beta$  ( $k_t(\beta)$  and so on) but  $k_c$  is determined at  $\beta = 0$ .

### 1.1 The connection of $\omega_{sn}(k)$ , $\omega_{sp}(k)$ , $\omega_{snp}(k)$ with solutions in SNM

A special attention is directed to the study of behavior of the branches at  $\beta \rightarrow 0$ . Here we need to define  $k_t(\beta)$ : this is the value of  $k$  when the branch goes under the cut and the real branch becomes complex. Studying the pass from ANM to SNM we have to consider separately the part of  $\omega_s(k)$  at small  $k$  ( $k < k_t$ ) when  $\omega_s(k)$  is real and the part at large  $k$  ( $k > k_t$ ) when  $\omega_s(k)$  is complex.

At  $k < k_t$  the real solutions smoothly change with  $\beta$  at  $-1 \leq \beta \leq 1$ . At  $\beta = 0$  we attribute them to  $\omega_s(k)$ , at  $\beta > 0$  attribute to  $\omega_{sn}(k)$  and to  $\omega_{sp}(k)$  at  $\beta < 0$ .

At  $k > k_t$  a branch  $\omega_{snp}(k)$  appears. It is a continuation of the complex part of  $\omega_s(k)$  to  $\beta \neq 0$ . The branch  $\omega_s(k)$  is a limit of a set of  $\omega_{snp}(k, \beta)$  at  $\beta \rightarrow 0$  at  $k > k_t$ .

In the limit  $\beta \rightarrow 0$  the branches  $\omega_{sn}(k)$  and  $\omega_{sp}(k)$  seem to come together and turn into the same branch. But our investigations demonstrate that the limit depends on  $k$  and is associated with  $k_c, k_t$  and  $\omega_{s1}(k)$ . At  $k < k_t$  this is really true. At  $k > k_c$  the branches  $\omega_{sn}(k)$  and  $\omega_{sp}(k)$  transit to  $\omega_{s1}(k)$  from the different unphysical sheets. But the limit  $\beta \rightarrow 0$  does not exist at  $k_t < k < k_c$  (Sect.4).

## 1.2 The connection of $\omega_{sn}(k)$ , $\omega_{sp}(k)$ , $\omega_{snp}(k)$ with solutions in NNM

We do not consider NNM as a  $\beta$ -stable nuclear matter, but the matter consisting on the neutrons only. Passing to the neutron matter the density of the proton states disappears at  $\beta \rightarrow 1$ . We must include this fact in calculation of solutions. We can do this redefining the density of states in the normalization factor of the effective interaction. The density of states  $N = d\rho/d\varepsilon_F$  is used in Eq.(6), it defines the factor  $C_0$ :  $C_0 = N^{-1} = \frac{\pi^2}{p_0 m_0}$ . We can define  $C_0$  through the density of states with the isospin of the  $ph$  pairs before and after the interaction.

$$C_{01,02} = (N_1 N_2)^{1/2} = \frac{\pi^2}{m_0 (p_{F1} p_{F2})^{1/2}}. \quad (3)$$

We repeat the reducing of the dispersion equation [8] with  $C_{01,02}$ . In SNM the results do not changed. But in ANM when  $\beta \rightarrow 1$  and  $p_{Fp} \rightarrow 0$  and we obtain that  $\omega_{sp}(k) \rightarrow 0$ ,  $\omega_{snp}(k) \rightarrow 0$ . Note, that  $\omega_{sp}(k)$  and  $\omega_{snp}(k)$  are the complex functions and both the real and imaginary parts go to zero. So in the neutron matter only the branch  $\omega_{sn}(k)$  survives and  $\omega_{sp}(k)$ ,  $\omega_{snp}(k)$  disappear. We demonstrate this in Sect.4.

In Sect. 2 we recall the system of equations for the effective vertexes which gives the dispersion equations [8]. In Sect. 3 we discuss the location of the solutions on the complex  $\omega$ -plane in SNM and ANM. In Sect. 4 we present the branches of solutions at the different  $\beta$ ,  $\rho = \rho_0$  and consider the behavior of branches at  $\beta \rightarrow 1$  and  $\beta \rightarrow 0$ .

## 2 Dispersion equation

We consider the isovector zero-sound excitations in the asymmetric nuclear matter. The equations for the effective fields which are the response of ANM to the external fields and can be written by analogy with the paper [8].

$$\begin{aligned} V_{eff}^{pp} &= V_0^p + F^{pp} A^p V_{eff}^{pp} + F^{pn} A^n V_{eff}^{np}, \\ V^{np} &= F^{np} A^p V_{eff}^{pp} + F^{nn} A^n V_{eff}^{np}, \\ V_{eff}^{nn} &= V_0^n + F^{nn} A^n V_{eff}^{nn} + F^{np} A^p V_{eff}^{pn}, \\ V_{eff}^{pn} &= F^{pp} A^p V_{eff}^{pn} + F^{pn} A^n V_{eff}^{nn}, \end{aligned} \quad (4)$$

$V_{eff}^{pp}$  ( $V_{eff}^{pn}$ ) is a component of the effective field which the proton feels when the external field  $V_0^\tau$  interacts with proton (neutron). We define  $V_{eff}^{np}$  ( $V_{eff}^{nn}$ ) by analogy.  $A^p$ ,  $A^n$  are the polarization operators. They are the integrals over the loops of the proton and the neutron particle-hole

excitations.

$$A^p = A^p(\omega, k) + A^p(-\omega, k), \quad A^n = A^n(\omega, k) + A^n(-\omega, k). \quad (5)$$

We use the effective Landau-Migdal interaction between the quasiparticles [9]

$$\mathcal{F}(\vec{\sigma}_1, \vec{\tau}_1; \vec{\sigma}_2, \vec{\tau}_2) = C_0 (F + F'(\vec{\tau}_1 \vec{\tau}_2) + G(\vec{\sigma}_1 \vec{\sigma}_2) + G'(\vec{\tau}_1 \vec{\tau}_2) (\vec{\sigma}_1 \vec{\sigma}_2)), \quad (6)$$

where  $\vec{\sigma}$ ,  $\vec{\tau}$  are the Pauli matrices in the spin and isospin spaces.  $C_0 = N^{-1} = \frac{\pi^2}{p_0 m_0}$  where  $N$  is the density of states of one sort of particles,  $m_0 = 0.94$  GeV. In [8, 9] the effective interaction between the similar (different) particles are  $F^{nn}$ , and  $F^{pp}$  ( $F^{np}$ ,  $F^{pn}$ ). They are associated with the constants in (6) by

$$F^{pp} = F^{nn} = C_0 (F + F'), \quad F^{pn} = F^{np} = C_0 (F - F'). \quad (7)$$

The matrix (4) we rewrite as

$$V_{eff} = V_0 + \mathcal{M} V_{eff}. \quad (8)$$

Here  $V_{eff}$  is a column, consisting from  $V_{eff}^l$ ,  $l = pp, pn, np, nn$ . The matrix  $\mathcal{M}$  is constructed from the elements  $F^{pp} A^p$ ,  $F^{pn} A^n$  and so on in (4). Reversing the matrix  $(1 - \mathcal{M})$  we obtain for  $V_{eff}$ :

$$V_{eff} = (1 - \mathcal{M})^{-1} V_0 = \frac{\tilde{\mathcal{M}}}{\det(1 - \mathcal{M})} V_0, \quad (9)$$

$\tilde{\mathcal{M}}$  is the adjoint matrix. We study the frequencies of the collective particle-hole excitations which correspond to the solutions to the dispersion equation  $\det(1 - \mathcal{M}) = 0$ .

$$\det(\omega, k) = (1 - F^{nn} A^n) (1 - F^{pp} A^p) - (A^p F^{pn}) (A^n F^{np}) \quad (10)$$

The dispersion equation for zero-sound frequencies is defined through the determinant of the matrix coupling the effective fields in matter and the external field [8]:

$$E(\omega, k) = 1 - C_0(F + F')A^p - C_0(F + F')A^n + 4FF'C_0^2 A^p A^n = 0. \quad (11)$$

We see that the isoscalar and isovector interactions contribute.

After integration over  $ph$ -loops we obtain for  $A^\tau(\omega, k)$  the expression in the form of the Migdal function [8] :

$$A^\tau(\omega, k) = -2 \frac{1}{4\pi^2} \frac{m^3}{k^3} \left[ \frac{a^2 - b_\tau^2}{2} \ln \left( \frac{a + b_\tau}{a - b_\tau} \right) - ab_\tau \right] \quad (12)$$

where  $a = \omega - (\frac{k^2}{2m})$ ,  $b_\tau = \frac{k p_{F\tau}}{m}$ .

## 2.1 Normalization of the effective interaction Eq.(6)

We investigate the solutions of (11) in the asymmetric nuclear matter. A special attention is paid to the study of solutions at  $\beta \rightarrow 0$  and  $\beta \rightarrow 1$ . When we transit to SNM we demonstrate the correspondence between the branches in SNM and ANM. In the neutron matter the density of the proton states goes to zero and we expect the disappearance of the branches  $\omega_{sp}(k)$  and  $\omega_{snp}(k)$ .

To include the dependence on the density of states we change the normalization of the effective quasiparticle interactions in the particle-hole channel by the following way:  $C_0 \rightarrow (C_{01}C_{02})^{1/2} = (N_1 N_2)^{-1/2}$  Eq.(3). We have included the density of states with the isospin of the  $ph$  pairs before and after the interaction. Then

$$F^{pp} = C_{0p} (F + F'), \quad F^{nn} = C_{0n} (F + F'), \quad (13)$$

$$F^{pn} = F^{np} = (C_{0p} C_{0n})^{1/2} (F - F').$$

Here  $C_{0p} = N_p^{-1} = \frac{\pi^2}{m_0 p_{Fp}}$ ,  $C_{0n} = N_n^{-1} = \frac{\pi^2}{m_0 p_{Fn}}$ . We repeat the derivation of the dispersion equation (11) with the redefined interaction (7) and obtain the following dispersion equation

$$E(\omega, k) = 1 - C_{0p}(F + F')A^p - C_{0n}(F + F')A^n + 4FF'C_{0p}C_{0n}A^pA^n = 0. \quad (14)$$

## 3 Location of solutions to Eqs. (11),(14)

In SNM we recall the main results on the energies of the particle-hole excitations [14, 15] and show the location of these results on the complex  $\omega$ -plane. Then we extend our consideration to ANM.

### 3.1 SNM

The system of equations (4) has two kinds of solutions corresponding to two sorts of excitations in nuclear matter: a set of the non-interacting particle-hole pairs  $\omega_{ph}(k)$  and the collective excitation  $\omega_s(k)$ . At the beginning we consider the solution of Eq. (11) in the symmetric nuclear matter. In this case  $A_p(\omega, k) = A_n(\omega, k) = A(\omega, k)$ ,  $A = A(\omega, k) + A(-\omega, k)$ . The dispersion equation (10) in SNM has the form:

$$\begin{aligned} E(\omega, k) &= (1 - F^{\tau\tau} A - F^{\tau\tau'} A) (1 - F^{\tau\tau} A + F^{\tau\tau'} A) = \\ &= (1 - 2C_0 F A) (1 - 2C_0 F' A) = 0. \end{aligned}$$

It separates in two factors and there are two branches  $\omega(k)$ : the branch generated by isoscalar effective interaction  $F$  and the second one generated by the isovector interaction  $F'$ . If  $F \neq F'$  the branches are separated.

Below we shall study solutions of Eq.(11) with  $F = 0$ .

$$1 - 2 C_0 F' A = 0. \quad (15)$$

This equation has the solutions corresponding to the collective excitations  $\omega_s(k)$ .

The excitation energies of the free noninteracting pairs are ( $p < p_F$  and  $|\vec{p} + \vec{k}| \geq p_F$ )

$$\omega_{ph}(k) = \varepsilon_{\vec{p}+\vec{k}} - \varepsilon_p, \quad \varepsilon_q = q^2/(2m). \quad (16)$$

We show the part of the energies of the free  $ph$ -pairs in Fig. 1 (*left*) as the dashed area. In SNM we can not distinguish the excitation of the neutron particle-hole pairs and the proton ones.

The branch of the collective excitations  $\omega_s(k)$  is shown by the solid curve in a schematic Fig. 1. We see that the collective excitation lies above the dashed area for the small  $k$ . At a definite  $k = k_t$  there is a overlapping of two modes. The solutions  $\omega_s(k)$  become complex because of the damping of the collective mode due to admixture of  $ph$ -mode. In Fig. 1 (*left*) at  $k > k_t$  only the real part  $\text{Re}\omega_s(k)$  is shown at the axis  $\omega > 0$  ( $\text{Im}\omega_s(k)$  is not shown).

We can consider  $\omega_s(k)$  and  $\omega_{ph}(k)$  from another point of view on the complex  $\omega$ -plane, Fig. 1 (*right*). The function  $A$  (5,12) has the logarithmic cuts. At a fixed  $k$  the cut of  $A(\omega, k)$  is shown in Fig. 1 (*right*) by the lines (1,1'). The cut of  $A(-\omega, k)$  correspond to the line (2,2').

$$(1, 1') : -\frac{kp_F}{m} + \frac{k^2}{2m} \leq \omega \leq \frac{kp_F}{m} + \frac{k^2}{2m}, \quad (2, 2') : -\frac{kp_F}{m} - \frac{k^2}{2m} \leq \omega \leq \frac{kp_F}{m} - \frac{k^2}{2m}. \quad (17)$$

The point of the cut are formed by the energies of the free  $ph$ -pairs  $\omega_{ph}$ .

The boundaries of  $\omega$  in (17) at  $\omega > 0$  are the boundary of the dashed area in Fig. 1 (*left*). At a fixed  $k$  the vertical line in the dashed area in Fig. 1 (*left*) corresponds to the cut (1-1') in Fig. 1 (*right*). The every point of the solid curve in Fig. 1 (*left*) at  $k < k_t$  (point  $A$ ) is the point on the real axis on the right from the cut in Fig. 1 (*right*). But the every point at  $k > k_t$  in Fig. 1 (*left*) (point  $B$ ) is the point under the cut on the nearest lower unphysical sheet of the Riemann surface of the logarithm in  $A(\omega, k)$  (12). The value  $k_t$  is determined by the condition that there is a solution to (15) such that  $\omega = \omega_s(k_t) = \frac{k_t p_F}{m} + \frac{k_t^2}{2m}$ , (see (17)). At large  $k$  we obtain on the unphysical sheet the complex solutions with  $\text{Re}\omega_s(k)$  larger then the end of the cut (17) (point  $C$ ) :  $\text{Re}\omega_s(k) \geq \frac{kp_F}{m} + \frac{k^2}{2m}$ .

To obtain the solutions in the overlapping region we must go under the cut to the unphysical sheet of  $A(\omega, k)$ . We are failed to find solution on the physical sheet of the complex  $\omega$ -plane at  $k > k_t$  [10, 11]. The transition of solutions of (11) to the unphysical sheet through the cut and appearance of their imaginary part we interpret as the damping of the collective excitations due to admixture of the free proton and neutron particle-hole pairs. In SNM we do not fix the isospin of the  $ph$  pairs. The branch  $\omega_s(k)$  is shown in Fig. 2 by the solid curves.



We have obtained the second collective branch of solutions to Eq. (11) (we denote it as  $\omega_{s1}(k)$ ). It is placed on the unphysical sheet of the functions  $A^p(\omega, k)$  or  $A^n(\omega, k)$  but not of the both:  $\omega_{s1}(k)$  is calculated on the unphysical sheet of the logarithm of  $A^n(\omega, k)$  but  $A^p(\omega, k)$  is taken on the lower half plane of the physical sheet of the complex  $\omega$ -plane. Changing  $n \leftrightarrow p$  we obtain the same  $\omega_{s1}(k)$  in SNM. This branch does not appear at the real axis. It is complex, damped quickly and started at some  $k = k_c$ . The value of  $k_c$  is obtained numerically. Branches of solutions  $\omega_s(k)$  and  $\omega_{s1}(k)$  are shown in Fig. 2. At the equilibrium density  $\rho = \rho_0$  we obtain  $k_c = 0.52 p_0$ ,  $k_t = 0.34 p_0$ . In calculations we use  $\rho_0 = 0.17 fm^{-3}$ ,  $p_0 = 0.268 GeV$ , isovector constant  $F'$  of the effective interaction Eq. (6) is  $F' = 1.0$ , effective nucleon mass  $m^* = 0.8 m_0$ .

### 3.2 ANM

In our model in asymmetric nuclear matter the excited collective states are damped due to mixture with  $ph$ -mode,  $\omega_{ph}^\tau$ . We can distinguish the mixture with  $\omega_{ph}^p(k)$ , with  $\omega_{ph}^n(k)$  and with  $\omega_{ph}^\tau(k)$ ,  $\tau = n, p$ . These three variants have the separate branches of solutions with the different widths.

In ANM the dispersion equation (14) has the form

$$1 - C_{0p} F' A^p - C_{0n} F' A^n = 0. \quad (18)$$

In Eq. (18) excitations  $\omega_{ph}^n(k)$  and  $\omega_{ph}^p(k)$  form the cuts in functions  $A^p$  and  $A^n$  (Eq. (5)) on the real axis.

The physical sheet and the cuts of Eq. (18) are shown in Fig. 3. The cuts of  $A^\tau(\omega, k)$  and  $A^\tau(-\omega, k)$  ( $\tau = n, p$ ) are:

$$(1, 1') : -\frac{kp_{F\tau}}{m} + \frac{k^2}{2m} \leq \omega \leq \frac{kp_{F\tau}}{m} + \frac{k^2}{2m}; \quad (2, 2') : -\frac{kp_{F\tau}}{m} - \frac{k^2}{2m} \leq \omega \leq \frac{kp_{F\tau}}{m} - \frac{k^2}{2m}. \quad (19)$$

The cut of  $A^\tau(\omega, k)$  is labeled by  $(1, 1')$  and the cut of  $A^\tau(-\omega, k)$  is labeled by  $(2, 2')$ . In Fig. 3 two sets of cut are shown for  $A^n$  and  $A^p$  when  $\beta > 0$  and  $p_{Fn} > p_{Fp}$ . In the symmetric nuclear matter the cuts are identical.

Now we consider solutions of Eq. (14) in the nuclear matter with  $\beta > 0$ . First, we obtain the zero-sound collective branch  $\omega_{sn}(k)$ . It is real at small  $k$ , then with  $k$  increasing it is overlapping with the set of the neutron  $ph$ -pairs ( $\omega_{ph}^n(k)$ ) and is damping due to the mixture with them. Since  $p_{Fn} > p_{Fp}$  the real solutions meet the neutron cut first and go under this cut. In nuclei this damping would correspond to the semi-direct decay of the collective state due to the neutron emission. Second, we obtain the zero-sound branch  $\omega_{sp}(k)$ . It is complex even at the small  $k$ , it is damping due to the mixture with the set of the proton  $ph$ -pairs ( $\omega_{ph}^p(k)$ ). In nuclei this damping would correspond to the decay of the collective state due to the proton emission. Third, there is a  $\omega_{snp}(k)$ , it is damping due to overlapping with nucleon  $ph$ -pairs (proton or neutron).

## 4 Solutions of the dispersion equation in ANM

At the beginning we compare the branches of solutions in SMN and in ANM with small  $\beta = 0.01$ . In Fig. 4a we show the same two curves as in Fig. 2 ( $\omega_s(k), \omega_{s1}(k)$ ) on the complex  $\omega$ -plane. In Fig. 4b,c,d we show the branches in ANM with a small  $\beta = 0.01$ :  $\omega_{sn}(k)$ ,  $\omega_{sp}(k)$ ,  $\omega_{snp}(k)$ . At small  $\beta$  the branches in ANM are close to that in SNM, but there is not the direct correspondence between the whole branches. It will be discussed below how the branches in ANM approximate the solutions in SNM and behave with  $\beta \rightarrow 0$ .

In Fig. 4 we see that the branches start at the different  $k$ . There are four wave vector values which are connected with branches, Fig.5:

- 1)  $k_t(\beta)$  - this is the value of wave vector when the real branch of solutions becomes complex. At  $\beta = 0$  the real solutions belong to  $\omega_s(k)$ , at  $\beta > 0$  - to  $\omega_{sn}(k)$  and at  $\beta < 0$  - to  $\omega_{sp}(k)$ .
  - 2)  $k_c$  is the wave vector value that the branch  $\omega_{s1}(k)$  starts (Fig. 2),  $k_c$  and  $\omega_{s1}(k)$  exist in SNM only.
  - 3)  $k_{1,2}^{np}(\beta)$  are connected with  $\omega_{snp}(k)$ ;  $k_1^{np}(\beta = 0) = k_t$ .  $k^{np}$  consists of two parts  $k_1^{np}$  and  $k_2^{np}$ . Solutions  $\omega_{snp}(k)$  exist at that  $\beta$  and  $k$  which are placed on the right and above the curve  $k^{np}(\beta)$ . There is not  $\omega_{snp}(k)$  on the left and below of the curve  $k^{np}(\beta)$ .
  - 4)  $k^p(\beta)$  is the beginning of  $\omega_{sp}(k)$  at  $\beta > 0$ . For the every  $\beta$   $\omega_{sp}(k)$  exist at  $k > k^p$ .
- We obtain that at  $\beta < 0.26$  there are inequalities  $k^p(\beta) < k_t(\beta) < k_1^{np}(\beta) < k_c$  which are very sensitive to the input values of  $F'$ ,  $m^*$ ,  $p_0$ .

To consider the solutions at  $\beta < 0$  we change the protons to neutrons and vice verse.

In the Figs. 6a – 6c and 7a – 7c the branches of solutions to Eq. (14)  $\omega_{sn}(k, \beta)$  (Fig. 6a),  $\omega_{sp}(k, \beta)$  (Fig. 6b) and  $\omega_{snp}(k, \beta)$  (Fig. 6c) are shown for the different asymmetry parameter  $\beta$ . Calculations are made for the density  $\rho = \rho_0$  and  $\beta = 0.01, 0.2, 0.5, 0.8$ .

### 4.1 The branches $\omega_{sn}(k, \beta)$

As it was mentioned above, at the small  $k$  and  $\beta > 0$  the dispersion equation has the real solutions. This takes place at  $k < k_t(\beta)$  (Fig. 5). We name them  $\omega_{sn}(k)$  because with  $k$  increasing there is overlapping of  $\omega_{sn}(k)$  with the neutron cut, Fig. 3 (point A). And  $\omega_{sn}(k)$  decay due to the mixture with the free neutron  $ph$  pairs.

After overlapping we continue the branch of solutions under the cut to the unphysical sheet of  $A^n(\omega, k)$ . It means that  $\text{Im}\omega_{sn}(k)$  appears at the wave vectors larger the definite one ( $k > k_t(\beta)$ ). The function  $k_t(\beta)$  is computed and shown in Fig. 5.

Dependence of  $\omega_{sn}(k)$  on  $\beta$  is shown in Fig. 6a. When the asymmetry parameter grows the real part of  $\omega_{sn}(k)$  increase. The dependence of  $|\text{Im}\omega_{sn}(k, \beta)|$  changes with  $k$ . We see the special

behavior of  $\omega_{sn}(k)$  at small  $\beta$ . This is explained by the transition to the solutions at  $\beta = 0$  which will be discussed below.

We can consider the real solutions  $\omega_{sn}(k)$  at  $k < k_t(\beta)$  as continuations to  $\beta \neq 0$  of the real solutions  $\omega_s(k)$  existing for  $\beta = 0$  and  $k \leq k_t(\beta = 0)$ .

## 4.2 The branches $\omega_{sp}(k, \beta)$

At  $\beta > 0$  the branch  $\omega_{sp}(k)$  is placed on the unphysical sheet completely. Since the real solution meets the neutron cut first when  $k$  increase (Fig. 3) we can not say that the real solution goes under the proton cut. We construct the unphysical sheet of  $A^p(\omega, k)$  similar to the sheet of  $A^n(\omega, k)$  and calculate the solutions on this sheet. This sheet is the nearest unphysical logarithmic sheet of the logarithm in  $A^p(\omega, k)$ . The imaginary part of  $\omega_{sp}(k)$  corresponds to the damping of excitation due to mixture with the proton free  $ph$ -pairs,  $\omega_{sp}(k)$  is complex at the every  $k$  for  $\beta > 0$ .

In the Figs. 6b and 7 the branches  $\omega_{sp}(k)$  are shown. The dependence of  $\omega_{sp}(k)$  on  $\beta$  differs from that of  $\omega_{sn}(k)$ : the real part of  $\omega_{sp}(k)$  decrease with  $\beta$ , but  $|\text{Im}\omega_{sp}(k)|$  increase. In the neutron matter ( $\beta = 1.0$ ), the branch  $\omega_{sp}(k)$  is absent, of course. A special behavior of  $\omega_{sp}(k)$  at  $\beta \rightarrow 1$ , when it turns to zero is discussed in Sect.4. As in Fig.6a, we see the special behavior of  $\omega_{sp}(k)$  at small  $\beta$ .

Our calculations show that  $\omega_{sp}(k)$  appears at the point  $k = k^p(\beta)$  (Fig. 5) and this  $\omega_{sp}(k^p)$  coincides with the proton cut point 2' in Fig.3 for  $A^p(-\omega, k)$  (17). Since at  $\beta > 0$  the branch  $\omega_{sp}(k)$  is completely placed under the proton cut of  $A^p(\omega, k)$ , we are forced to conclude that or 1)  $\omega_{sp}(k)$  at  $k < k^p$  is placed under the both (1,1') and (2,2') cuts in Fig.3 for  $A^p$  and we must take into account  $2p2h$  states, or 2) accept that at  $k < k^p$  the collective excitation  $\omega_{sp}(k)$  annihilates with  $ph$  pairs. Decision is in progress.

## 4.3 The branches $\omega_{snp}(k, \beta)$

The branch  $\omega_{snp}(k, \beta)$  is formed by the solutions of Eq.(18). This equation coincides with Eq.(15) if  $\beta = 0$ . As it discussed above, Eq.(15) has a branch of solutions  $\omega_s(k)$ , they are real at  $k \leq k_t$  and complex at  $k > k_t$ . The branch  $\omega_{snp}(k, \beta)$  is defined as continuation of the complex part of  $\omega_s(k)$  to  $\beta \neq 0$ .

In Fig. 6c and 7 we show  $\omega_{snp}(k)$  for different  $\beta > 0$ . At  $\beta > 0$   $\omega_{snp}(k)$  starts at  $k = k^{np}$  and is placed on the unphysical sheets only. At  $\beta = 0$  we have  $k_t = k^{np}$  (Fig. 5).

As it is shown in Fig.5 the function  $k^{np}(\beta)$  consist of two parts  $k_1^{np}(\beta)$  and  $k_2^{np}(\beta)$ . The behavior of  $\omega_{snp}(k)$  (shown in Fig.8) explains the behavior of  $k^{np}(\beta)$ . At  $\beta < 0.26$  there is no solutions at small  $k$ , they exist at  $k \geq k_1^{np}(\beta)$  only. But at  $0.26 \leq \beta \leq 0.36$  the branch  $\omega_{snp}(k, \beta)$

consists of two parts. For example, at  $\beta = 0.3$  (Fig. 8) the first part exists at  $0 \leq k \leq k_2^{np}(\beta)$  and the second one at  $k > k_1^{np}(\beta)$ . For  $\beta > 0.36$  the branch  $\omega_{snp}(k, \beta)$  exists at all (relevant to our approach). The imaginary part of  $\omega_{snp}(k, \beta)$  corresponds to the decay of  $\omega_{snp}(k)$  due to mixture with nucleon  $ph$  pairs, but isospin of these pairs is not fixed unlike  $\omega_{sn}(k)$  and  $\omega_{sp}(k)$ .

#### 4.4 Behavior of solutions at $|\beta| \rightarrow 1$

As it was explained in Introduction, we wait a special behavior of solutions at  $\beta > 0$  and  $p_{Fp} \rightarrow 0$  (and  $\beta < 0$  and  $p_{Fn} \rightarrow 0$ ). As the density of the proton states go to zero we wait disappearance of  $\omega_{sp}(k)$  and  $\omega_{snp}(k)$ . To take into account the decreasing of the density of the proton states we change the normalization of the effective interaction, Eq.(13). The dispersion equation for the zero sound in ANM is presented in Eq.(14). In this subsection we compare solutions at  $|\beta| \sim 1$  of the Eqs.(11) and (14).

The presentation of results is given in Fig. 9. We fix  $k = p_0$  and change the asymmetry parameter  $\beta$ . The numbers 1 and 2 denote the solutions of Eqs.(11) and (14), correspondingly. We see that  $\omega_{sp}(k)$  and  $\omega_{snp}(k)$  marked by 2 turn to zero at  $\beta \rightarrow 1$  and only  $\omega_{sn}(k)$  survives in Eq.(14). But the solutions of Eq.(11) do not disappear at  $|\beta| \rightarrow 1$ . We obtain the nonzero solutions and this contradict to the physical picture at  $\beta \rightarrow 1$ .

#### 4.5 Behavior of solutions at $|\beta| \rightarrow 0$

We demonstrate the behavior of branches  $\omega_s(k)$ ,  $\omega_{s1}(k)$ ,  $\omega_{sn}(k)$ ,  $\omega_{sp}(k)$  and  $\omega_{snp}(k)$  at small  $|\beta|$ . We consider  $\beta > 0$  mainly.

At  $\beta = 0$  in SNM we have 2 branches  $\omega_s(k)$  and  $\omega_{s1}(k)$  (Fig. 2). Fig. 4 is made for small  $\beta = 0.01$ . In this figure we see redistribution of  $\omega_s(k)$  and  $\omega_{s1}(k)$  by  $\omega_{sn}(k)$ ,  $\omega_{sp}(k)$  and  $\omega_{snp}(k)$ . At  $k \leq k_t(\beta)$  (on the left of '1', Fig. 4a)  $\omega_s(k)$  passes into  $\omega_{sn}(k)$  (compare figures *a* and *b*). At  $k > k_t(\beta)$  (on the right of '1', Fig. 4a)  $\omega_s(k)$  transits to  $\omega_{snp}(k)$  (compare figures *a* and *d*). In figures *a*, *b*, *c* the branch  $\omega_{s1}(k)$  looks like splitting on  $\omega_{sn}(k)$  and  $\omega_{sp}(k)$  which are placed on the different unphysical sheets.

At first, we consider the dependence of the real solutions of Eq.(14) on  $\beta$ . They are shown at  $k < k_t(\beta)$  in Figs. 2, 4(*a, b*), 5. The real solutions are the lines started at  $k = 0$  and  $\omega = 0$  and finished at  $k = k_t(\beta)$  and  $\omega(k_t, \beta)$  (Fig. 5). We attribute them at  $\beta = 0$  to  $\omega_s(k)$ :  $\omega(k, \beta) = \omega_s(k, \beta = 0)$  and at  $\beta > 0$  to  $\omega_{sn}(k, \beta)$ :  $\omega(k, \beta) = \omega_{sn}(k, \beta > 0)$ . We see that there is the continuous transition with change of  $\beta$  between the different kinds of branches at  $k \leq k_t(\beta)$ . The branch  $\omega_{sn}(k, \beta)$  is the continuation of the real part of  $\omega_s(k)$  to  $\beta \neq 0$ , Figs. 4, 5.

In Fig. 10 the solutions are shown on the complex  $\omega$ -plane. This presentation is a very sensitive

to the distinction of branches. The branch  $\omega_{s1}(k)$  shown by the solid curve in Fig. 10a, corresponds to the dashed curve in Fig. 4a. In Fig. 10a we see that the branches  $\omega_{sn}(k)$  and  $\omega_{sp}(k)$  calculated for  $\beta=0.01$  envelope  $\omega_{s1}(k)$  (number '1'). This is more expressive for smaller  $\beta$  (but difficult to draw since they are too close). For the larger  $\beta$ :  $\beta = 0.1$  (number '2'), the branches do not feel  $\omega_{s1}(k)$  at all. This explains the distinct behavior of these branches at small  $\beta$ , Figs. 6, 7. So we conclude that  $\omega_{s1}(k)$  is the limit of  $\omega_{sn}(k)$  and  $\omega_{sp}(k)$  at  $\beta \rightarrow 0$  (from different unphysical sheets). This is true at  $k > k_c$  when  $\omega_{s1}(k)$  exists since we do not obtain at  $\beta = 0$  and  $k < k_c$  the solutions of the kind  $\omega_{sn}(k)$  or  $\omega_{sp}(k)$ .

Now let consider the branch  $\omega_{snp}(k)$ , which by definition is the continuation of the complex part of  $\omega_s(k)$  to  $\beta \neq 0$ . In Fig. 10b we show a part of Fig. 8 (adding the branch at  $\beta=0.1$ ). At small  $\beta$  the branches  $\omega_{snp}(k)$  start at  $k_1^{np}(\beta)$  (see Fig. 5) and  $k_1^{np}(\beta) \rightarrow k_t(\beta = 0)$  when  $\beta \rightarrow 0$ . In Fig. 10b we see that at  $\beta \rightarrow 0$  branches  $\omega_{snp}(k)$  go to  $\omega_s(k)$  (solid curve). We check numerically that the complex part of  $\omega_s(k)$ , appearing at  $k > k_t(\beta = 0)$  is really a limit of  $\omega_{snp}(k, \beta)$  at  $\beta \rightarrow 0$ .

Our results demonstrate how the solutions at  $\beta = 0$ :  $\omega_s(k)$ ,  $\omega_{s1}(k)$  are continued to  $\beta \neq 0$ . We consider  $\omega_s(k)$  as consisting of two parts: real (at  $k \leq k_t$ ) and complex (at  $k \geq k_t$ ). At  $\beta > 0$  the real part turns into the real part of  $\omega_{sn}(k, \beta)$  but the complex part turns into  $\omega_{snp}(k, \beta)$ . The branch  $\omega_{s1}(k)$  exist at  $k > k_c$  and is continued at  $\beta \neq 0$  into two unphysical sheets, splitting into  $\omega_{sn}(k, \beta)$  and  $\omega_{sp}(k, \beta)$ . One unphysical sheet belongs to  $A^n(\omega, k)$ , the second one to  $A^p(\omega, k)$ , Eq.(12).

## 4.6 Presentation of the solutions at $-1 \leq \beta \leq 1$

In this section we demonstrate the behavior of solutions  $\omega_{sn}(k, \beta)$ ,  $\omega_{sp}(k, \beta)$ ,  $\omega_{snp}(k, \beta)$  when asymmetry parameter changes  $-1 \leq \beta \leq 1$  (Figs. 11, 12). Our investigations indicate that the behavior is various for the branches of the different kind and depends on value of  $k$ .

Now we give the total picture for behavior of branches  $\omega_{sn}(k, \beta)$ ,  $\omega_{sp}(k, \beta)$  at  $-1 \leq \beta \leq 1$ , Figs. 11. We explained above that there are the specific values of the wave vector  $k_t(\beta)$ ,  $k^p(\beta)$ ,  $k_c$ ,  $k^{np}(\beta)$ , Fig. 5, which determine the changes of branches on  $\beta$ . In Fig. 11 we demonstrate  $\beta$ -dependence of the real and imaginary parts of branches  $\omega_{sn}(k)$ ,  $\omega_{sp}(k)$  at some values  $k_1 = 0.05p_0$ ,  $k_2 = 0.4p_0$ ,  $k_3 = 0.6p_0$  in the three different intervals:  $k_1 < k_t(\beta)$ ,  $k_t(\beta) < k_2 < k_c$  and  $k_3 > k_c$ .

In the upper part of Fig. 11 the real parts of solutions are shown. At  $k = k_1$  and  $\beta > 0$  the branch  $\omega_{sn}(k_1)$  is real. Changing  $\beta$  from  $\beta = 1$  to negative values we go to the real  $\omega_{sp}(k_1)$  at  $\beta < 0$ . At  $\beta = 0$  the branch goes through the point  $\omega_s(k_1)$ . At  $k = k_1$  and  $\beta > 0$  the branch  $\omega_{sp}(k_1)$  is complex, it does not exist (at least, it is not found) at  $k < k^p(\beta)$  and can not be continued to negative  $\beta$ . The same we can say at  $\beta < 0$  about  $\omega_{sn}(k_1)$  which can not be continue to positive  $\beta$ .

We are interesting to know all physical solutions in our model at  $k = k_A$  and  $\beta = \beta_A$ . So it is important to know is  $\omega_{sp}(k_1)$  at  $\beta = \beta_A$  a physical solution? Can we do the analytical continuation from physical solution  $\omega_{sn}(k_1, \beta_A)$  to  $\omega_{sp}(k_1, \beta_A)$ ? The answer will be presented below.

At  $k = k_2$  and  $\beta > 0$  the branch  $\omega_{sn}(k_2)$  is complex, Figs.6,7. As explained above we can not continue it to  $\omega_{sp}(k_2)$  changing  $\beta$  from the positive to negative values. There is the discontinuity in dependence of the solutions on  $\beta$  at  $\beta = 0$  and  $k = k_2$ . From the technical point of view: at these  $k$  there are not solutions of Eq.(18) of  $\omega_{sn}(k)$ ,  $\omega_{sp}(k)$  kind. From the physical point of view: excitations at these  $k$  ( $k_t(\beta) < k_2 < k_c$ ) looks like two different phases at  $\beta > 0$  and  $\beta < 0$  and there is a phase boundary at these  $k$ .

Both at  $k = k_1$  and  $k = k_2$  we can not associate  $\omega_{sp}(k_2, \beta > 0)$  with  $\omega_{sn}(k_2, \beta < 0)$  changing  $\beta$  only.

At  $k = k_3$  and  $\beta > 0$  the branch  $\omega_{sn}(k)$  is a complex one but we have a complex solution at  $\beta = 0$  ( $\omega_{s1}(k_3)$ ). We can move  $\beta$  to negative values and continue  $\omega_{sn}(k_3, \beta > 0)$  to  $\omega_{sp}(k_3, \beta < 0)$  through the point  $\omega_{s1}(k_3)$ . Moreover we can do the analytical continuation from physical solution  $\omega_{sn}(k_3, \beta_A)$  to  $\omega_{sp}(k_3, \beta_A)$  at the same  $\beta_A$  through this point. In figure we see that we can continue  $\omega_{sn}(k_3, \beta)$  from  $\beta = \beta_A$  to  $\beta = 0$  and  $\omega_{sn}(k_3, \beta) \rightarrow \omega_{s1}(k_3)$ , then we transit  $\omega_{s1}(k_3) \rightarrow \omega_{sp}(k_3, \beta_A)$ .

As a result we have a receipt how to know whether  $\omega_{sp}(k_1)$  is the physical solution at  $\beta_A$  ( $k_1 > k^p(\beta)$ ). We do continuation of  $\omega_{sn}(k_1, \beta_A)$  from  $k_1$  to  $k_3$ , then transit to  $\omega_{sp}(k_3, \beta_A)$ , and changing  $k$  go back to  $\omega_{sp}(k_1, \beta_A)$ . We are able to do the analytical continuation and conclude that  $\omega_{sp}(k_1)$  is a physical solution.

Return to  $k = k_2$ . Since there are not continuation on  $\beta$  for  $k$  in the interval  $k_t < k < k_c$  we must go around the point  $k = k_c$ :  $\omega_{sn}(k_2, \beta_A) \rightarrow \omega_{sn}(k_3, \beta_A) \rightarrow \omega_{s1}(k_3) \rightarrow \omega_{sp}(k_3, \beta_A) \rightarrow \omega_{sp}(k_2, \beta_A)$ .

In Fig. 11 (lower part) the imaginary parts of branches  $\omega_{sn}(k, \beta)$ ,  $\omega_{sp}(k, \beta)$  for the same  $k_1, k_2, k_3$  are shown. At  $k = k_1$  the branch  $\omega_{sn}(k, \beta)$  is real by the definition of  $k_1$  and passes into the real  $\omega_{sp}(k, \beta)$  when  $\beta$  goes to negative values. At  $\beta > 0$   $\text{Im}\omega_{sp}(k_1, \beta)$  is very small (see Sect.(4.2)) and tends to zero at  $k \rightarrow k^p$  (but does not reach it since it exists at the unphysical sheet). At  $k = k_2$  at  $|\beta| \rightarrow 0$  the imaginary parts of branches go to zero, but do not reach the point  $\beta = 0$  since there are not solutions of the dispersion equation at  $\beta = 0$  for these  $k$ , Fig. 2. At  $k = k_3$   $\text{Im}\omega_{sn}(k, \beta)$  transit to  $\text{Im}\omega_{sp}(k, \beta)$  when we move  $\beta$  to negative values. And we can go for a given  $\beta_A$  from  $\text{Im}\omega_{sn}(k, \beta_A)$  to  $\text{Im}\omega_{sp}(k, \beta_A)$  similar to the real parts.

In Figs.11 for every  $k$  we see how the real and imaginary parts of  $\omega_{sp}(k, \beta)$  ( $\omega_{sn}(k, \beta)$ ) go to zero when  $\beta \rightarrow 1$  ( $\beta \rightarrow -1$ ).

In Fig. 12 we present the dependence of  $\omega_{snp}(k, \beta)$  on  $\beta$  at three different values  $k_1 = 0.3 p_0$ ,  $k_2 = 0.355 p_0$ ,  $k_3 = 0.4 p_0$ . Looking at the curve  $k^{np}(\beta)$  in Fig. 5 we expect the different dependence of

$\omega_{snp}(k, \beta)$  on  $\beta$  at these  $k_{1,2,3}$  since  $k_1 < k_t(\beta)$ ,  $k_t < k_2 < k_1^{np}(max)$  and  $k_3 > k_1^{np}(max)$ . In Figs. 12 we see that at  $k = k_1$  the branch  $\omega_{snp}(k)$  starts at  $\beta > \beta_1$  where  $k_1^{np}(\beta_1) = k_1$ . This correspond to Fig. 5: there is not solutions on the left and below the curve  $k_1^{np}(\beta)$ . At  $k = k_2$  there are two parts of solutions: at a small  $\beta \simeq 0.02$  and  $\beta > \beta_2$ , where  $k_1^{np}(\beta_2) = k_2$ . In Fig. 12 the small part of solutions is shown at small  $\beta$  and the main part at  $\beta > \beta_2$ . At  $k = k_3$  we have solutions at all  $\beta$  (see Figs. 5,8). So when we go from positive  $\beta$  to negative ones, the branch  $\omega_{snp}(k)$  transits to  $\omega_{spn}(k)$  crossing the point  $\omega_s(k = 0.4p_0)$  at  $\beta = 0$ . See Figs. 12 for the real and imaginary parts (solid curves).

As a result, at  $k = k_3$  we have solutions at all  $\beta$ . At  $k = k_1$  there are not solutions for small  $\beta$  and there is a broken dependence of  $\omega_{snp}(k, \beta)$  at  $k = k_2$ . In all cases we see that  $\omega_{snp}(k, \beta)$  and  $\omega_{spn}(k, \beta)$  go to zero at  $|\beta| \rightarrow 1$ .

## 5 Summary

We consider nuclear matter with asymmetry parameter  $-1 \leq \beta \leq 1$ . We obtain the complex branches of the solutions of the dispersion equation (14). The imaginary part of them describes the decay of zero-sound excitations due to an admixture of the free particle-hole pairs (of a corresponding kind) into the collective excitations.

The symmetric, asymmetric and neutron matter are considered. In SNM we obtain two branches of solutions  $\omega_s(k, \beta = 0)$  and  $\omega_{s1}(k, \beta = 0)$  (Fig. 2). In ANM three branches are found:  $\omega_{sn}(k, \beta)$ ,  $\omega_{sp}(k, \beta)$  and  $\omega_{snp}(k, \beta)$  for every  $-1 < \beta < 1$  (Figs. 6,7) and one branch in neutron matter  $\omega_{sn}(k, \beta = 1)$  (Fig. 9,11). During the calculations, the branches naturally appear as result of attempt to connect solutions of the dispersion equation Eq. (14) for different  $\beta$ . The changes of solutions with  $\beta$  depend on the value of wave vectors. There are four values of  $k$  which determine the different regions. For small  $\beta$  we have  $k^p(\beta) < k_t(\beta) \leq k_1^{np}(\beta) < k_c$  (Fig. 5).

At  $k < k_t(\beta)$  solutions are real and can be calculated for all  $\beta$  (Fig. 11) and it is easy to pass from one  $\beta$  to another. We attribute solutions to the branches of the different kind: for  $\beta = 0$  to  $\omega_s(k)$ , for  $\beta > 0$  to  $\omega_{sn}(k)$  and to  $\omega_{sp}(k)$  for  $\beta < 0$ . At  $k > k_t(\beta)$  solutions become complex. An additional branch  $\omega_{snp}(k)$  is obtained. It is the continuation of  $\omega_s(k)$  to  $\beta \neq 0$  at  $k > k_t(\beta)$ .

We investigated the behavior of branches when  $|\beta| \rightarrow 0$  and  $|\beta| \rightarrow 1$ . It is shown that at  $\beta \rightarrow 1$  the branches  $\omega_{sp}(k)$  and  $\omega_{snp}(k)$  go to zero. Only  $\omega_{sn}(k)$  survives. We obtain this result in our calculations if to take into account the decreasing to zero of the proton states density at  $\beta \rightarrow 1$  (Eq. (3)).

At  $\beta \rightarrow 0$  and  $k > k_t$  the complex part of  $\omega_s(k)$  is the limit of the set of branches  $\omega_{snp}(k, \beta)$ . When  $\beta \rightarrow 0$  and  $k > k_c$  the branches  $\omega_{sp}(k)$  and  $\omega_{sn}(k)$  go to  $\omega_{s1}(k)$ . At  $k_t < k < k_c$  there is not

the limit of  $\omega_{sn}(k)$  and  $\omega_{sp}(k)$  for  $\beta \rightarrow 0$ . The excitations look similar to the difference phases.

The results presented above can be applied to the investigation of the response functions of the nuclear matter and nuclei. Note, that our results are very sensitive to the density [11] and the quasiparticle interactions (even taken in the simple form Eq.(6)). The inclusion of the isoscalar interaction  $F$  changes essentially the figures 5,8 and 12.



## References

- [1] Lipparini Enrico, Pederiva Francesco, Phys. Rev. **C 88**, 024318 (2013).
- [2] K. Morawetz, U. Fuhrmann, and R. Walke, Phys. Rev. **C 58**, 1473 (1998).
- [3] K. Morawetz, U. Fuhrmann, and R. Walke, in Isospin Effects in Nuclei, edited by B. A. Lie and U. Schroeder (World Scientific, Singapore, 2000), chap. 7, correct version: nucl-th/0001032.
- [4] Kolomietz V.M., Shlomo S., Phys.Rev. **C 64**, 044304 (2001).
- [5] M. di Toro, V.M. Kolomietz, A.B. Larionov, Phys. Rev. **C 59**, 3099 (1999).
- [6] F. L. Braghin, D. Vautherin, A. Abada , Phys. Rev. **C 52**,2504 (1995).
- [7] Greco V., Colonna M., Di Toro M., Matera F., Phys. Rev. **C 67**, 015203 (2003).
- [8] Migdal A.B., Zaretsky D.F., Lushnikov A.A., Nucl. Phys. **A 66**, 193 (1965).
- [9] Migdal A., Voskresenskii D.N., Saperstein E.E., and Troitskii M.A., Phys. Rep. **192**, 179 (1990).
- [10] Sadovnikova V.A., Phys. Atom. Nucl. **70**, 989 (2007).
- [11] Sadovnikova V.A., Bull. Russ. Acad. Sci. Phys., **78**, 853 (2014); **81**, 1196 (2017)
- [12] R.G. Newton, *Scattering theory of waves and particles*, McGRAW-HILL COMPANY, 1969.
- [13] P. Ring, P. Schuck, “*The nuclear many-body Problem*”,Springer-Verlag,1980.
- [14] J.W. Negele, H. Orland, *Quantum Many-Particle Systems*, (Westview Press, 1998).
- [15] L.S. Levitov, A.B. Shitov, “*Green functions*”, (M. Fizmatlit, 2002).

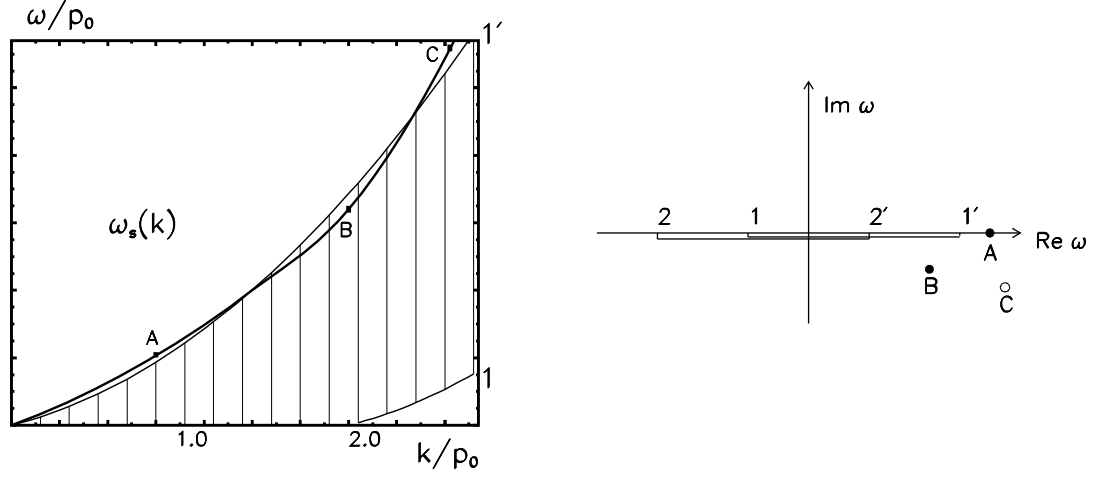


Figure 1: A schematic figure. *left*: The solid curve presents  $\omega_s(k)$ . The dashed area is occupied by the free  $ph$  pairs  $\omega_{ph}$  corresponding to the cut (1-1'). *right*: The cuts of the function A in (5,12). The cut (1-1') is the cut of  $A(\omega, k)$ . The cut (2-2') is the cut of  $A(-\omega, k)$ . The point A, B, C mark the solutions having the different location in respect to the cuts.

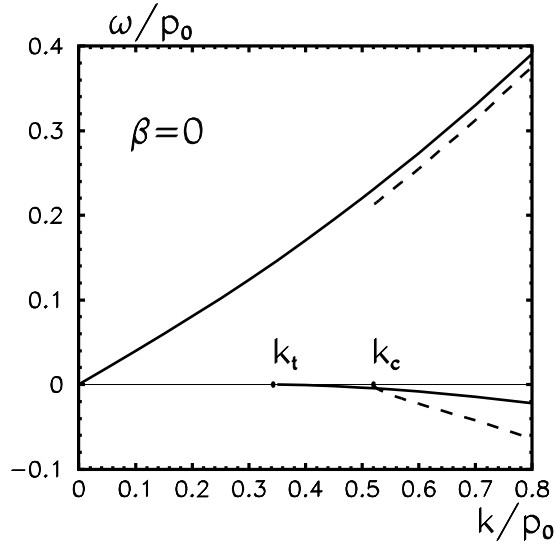


Figure 2: The branches of solutions in SNM. The solid curves is for  $\omega_s(k)$ , the dashed curves -  $\omega_{s1}(k)$ . At  $\omega > 0$  we place  $\text{Re } \omega_s(k)$ ,  $\text{Re } \omega_{s1}(k)$ . At  $\omega < 0$  there are placed the imaginary parts of branches.

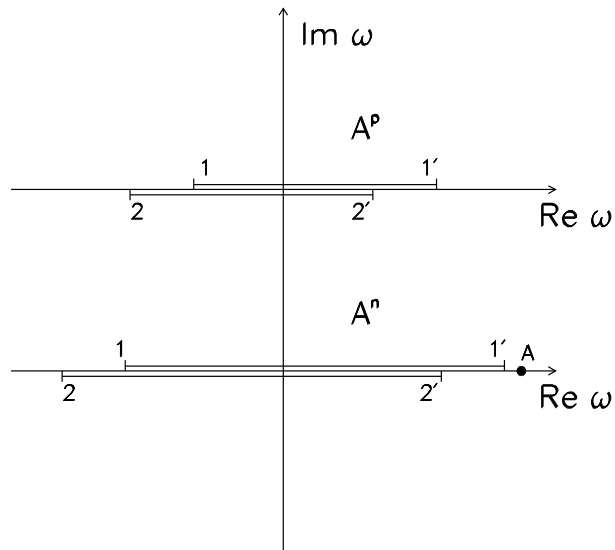


Figure 3: A schematic figure at  $\beta > 0$ . The cuts of the functions  $A^\tau$  (12) are presented on the complex  $\omega$ -plane. The cut (1-1') is the cut of  $A^\tau(\omega, k)$ . The cut (2-2') is the cut of  $A^\tau(-\omega, k)$ . In the upper (lower) part the cuts of  $A^p$  ( $A^n$ ) are demonstrated.

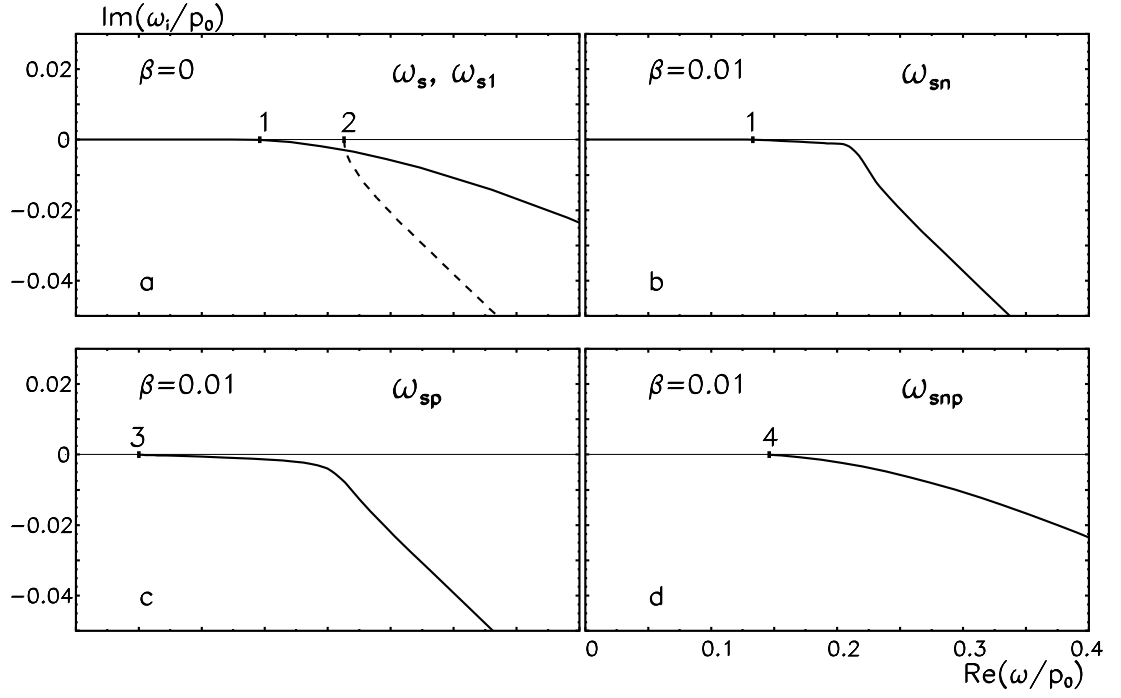


Figure 4: Comparison of zero-sound solutions in SNM and in ANM for small  $\beta$ . The complex  $\omega$ -plane: at the horizontal axis we show  $\text{Re } \omega_{si}(k)$ , at the vertical axis -  $\text{Im } \omega_{si}(k)$ . (a):  $\beta = 0$ , solid curve is  $\omega_s(k)$ , dashed curve is  $\omega_{s1}(k)$ ; point '1' marks  $\omega_s(k_t)$ , '2' is for  $\omega_{s1}(k_c)$ . (b):  $\beta = 0.01$ , the branch  $\omega_{sn}(k)$ , '1' stands for  $\omega_{sn}(k_t)$ . (c):  $\beta = 0.01$ , the branch  $\omega_{sp}(k)$ , point '3' shows  $\omega_{sp}(k^p)$ . (d):  $\beta = 0.01$ , the branch  $\omega_{snp}(k)$ , '4' -  $\omega_{snp}(k^{np})$ .

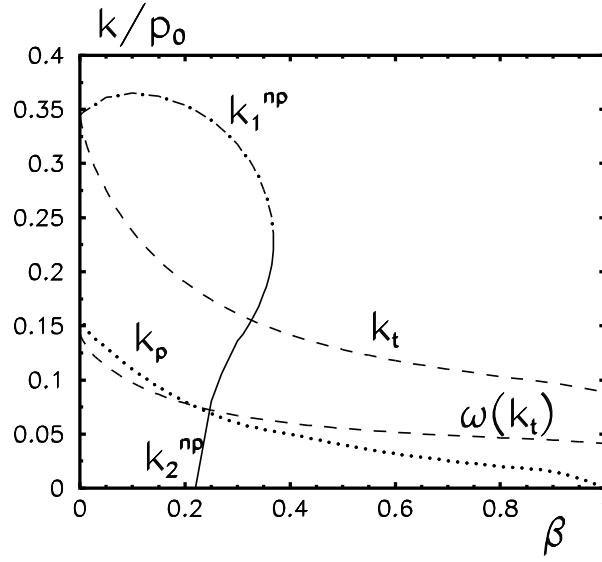


Figure 5: Dependence of a special wave vector values  $k_t(\beta)$ ,  $k^p(\beta)$ ,  $k^{np}(\beta)$  on  $\beta$ . The curve  $k^{np}(\beta)$  consists from two parts:  $k_2^{np}(\beta)$  (solid curve) and  $k_1^{np}(\beta)$  (dash-dotted curve). The dashed curves is for  $k_t(\beta)$ ; dotted curves -  $k^p(\beta)$ ;  $\omega(k_t)$  is the final point of the real solutions at different  $\beta$ . The curves can be symmetrically reflected to the negative  $\beta$ .

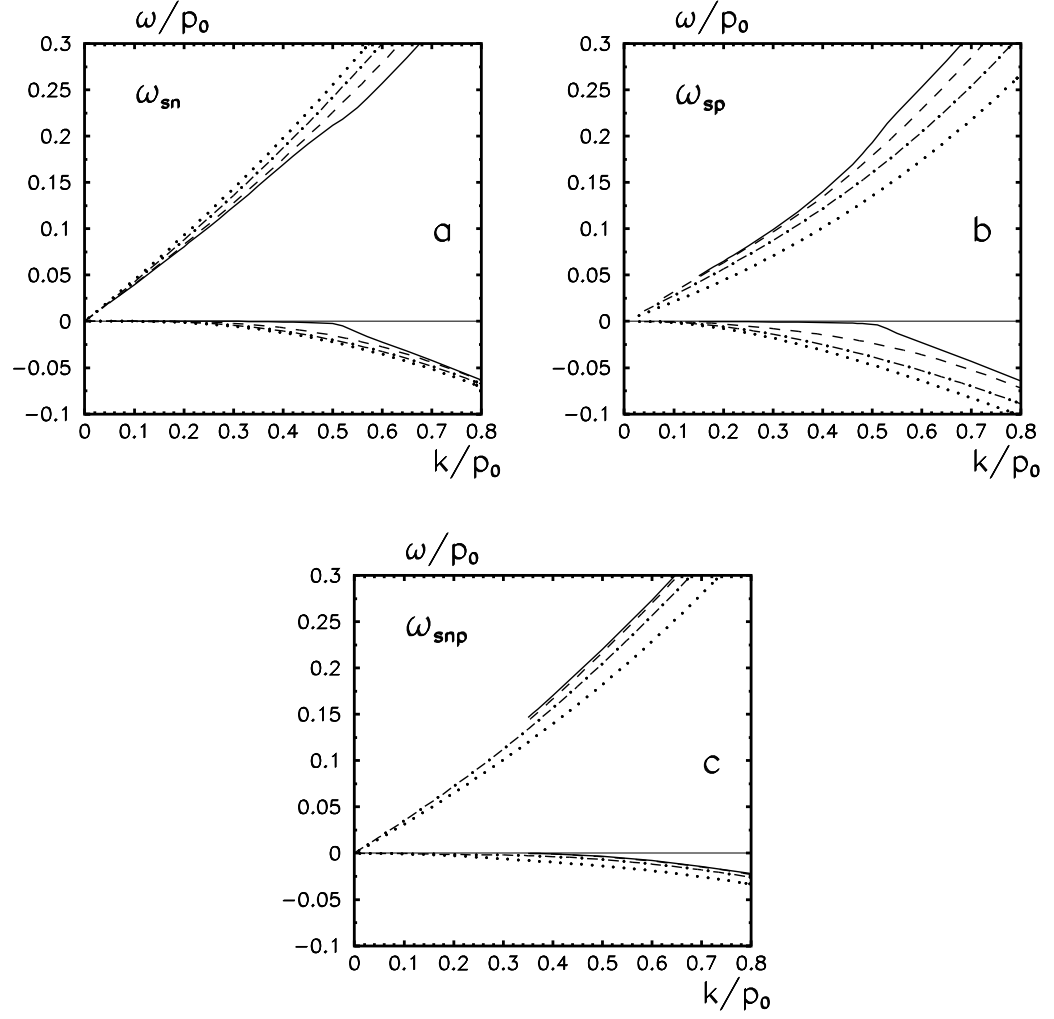


Figure 6: Dependence of the branches  $\omega_{sn}(k)$  (a),  $\omega_{sp}(k)$  (b) and  $\omega_{snp}(k)$  (c) on  $\beta$ . At  $\beta=0.01$  – solid curves; 0.2 – dashed; 0.5 – dot-dashed; 0.8 – dotted. Other notations are the same as in Fig. 2.

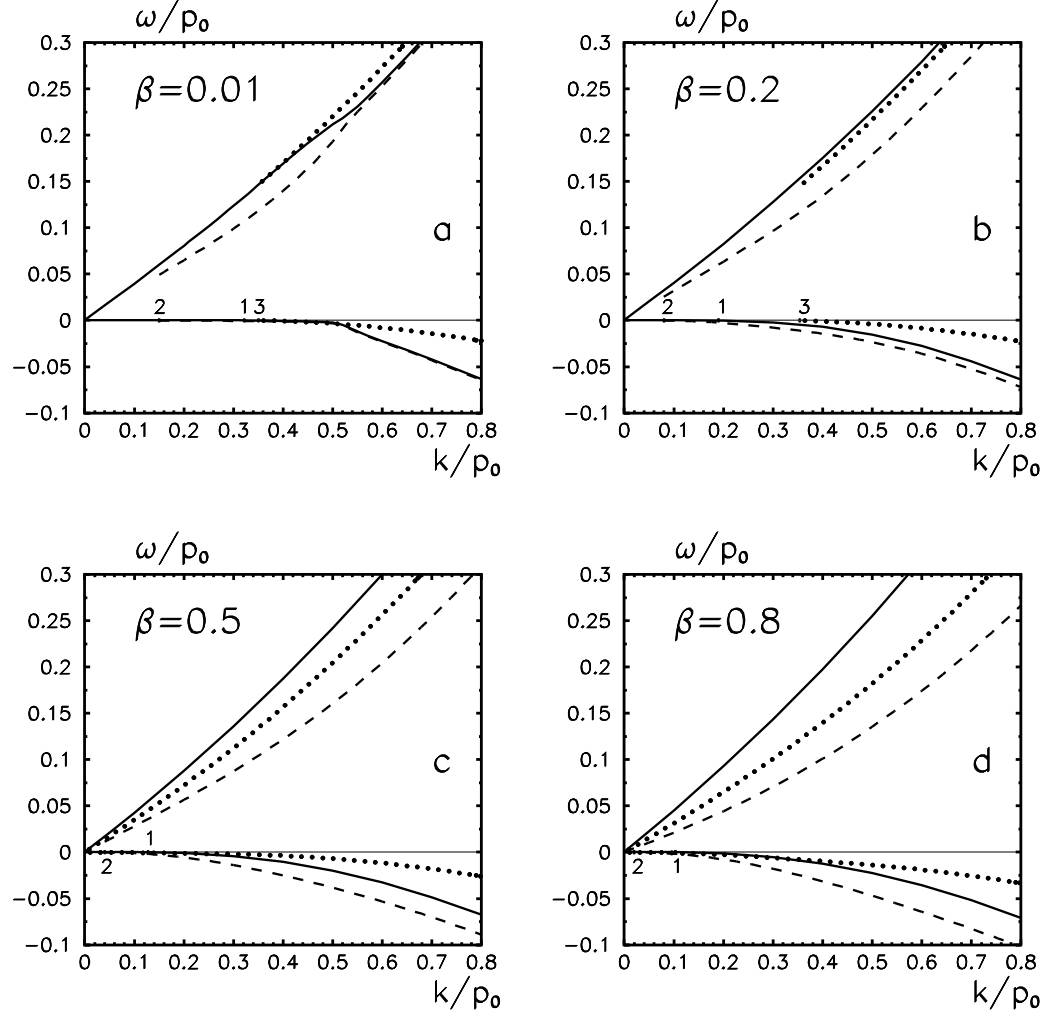


Figure 7: Comparison  $\omega_{sn}(k)$ ,  $\omega_{sp}(k)$  and  $\omega_{snp}(k)$  for different  $\beta$ :  $\beta=0.01$  (a),  $0.2$ (b),  $0.5$ (c),  $0.8$ (d).  $\omega_{sn}(k)$  are shown by the solid curves; dashed curves show  $\omega_{sp}(k)$ ; dotted curves -  $\omega_{snp}(k)$ . The number '1' means wave vector  $k_t/p_0$ , the number '2' -  $k^p/p_0$ , '3' -  $k^{np}/p_0$ . Other notations are the same as in Fig. 2.

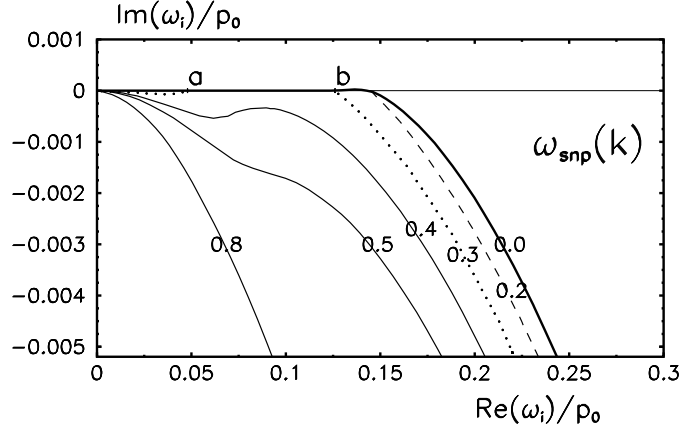


Figure 8: Branches  $\omega_{snp}(k, \beta)$ . Complex  $\omega$ -plane. The values of  $\beta$  is shown on the every curve. Solid bold curve stands for  $\omega_s(k)$ ,  $\beta = 0$ . For  $\beta = 0.3$  the points  $a$  and  $b$  stand for  $a = \omega_{snp}(k_2^{np})$ ,  $b = \omega_{snp}(k_1^{np})$  (see Fig. 5).

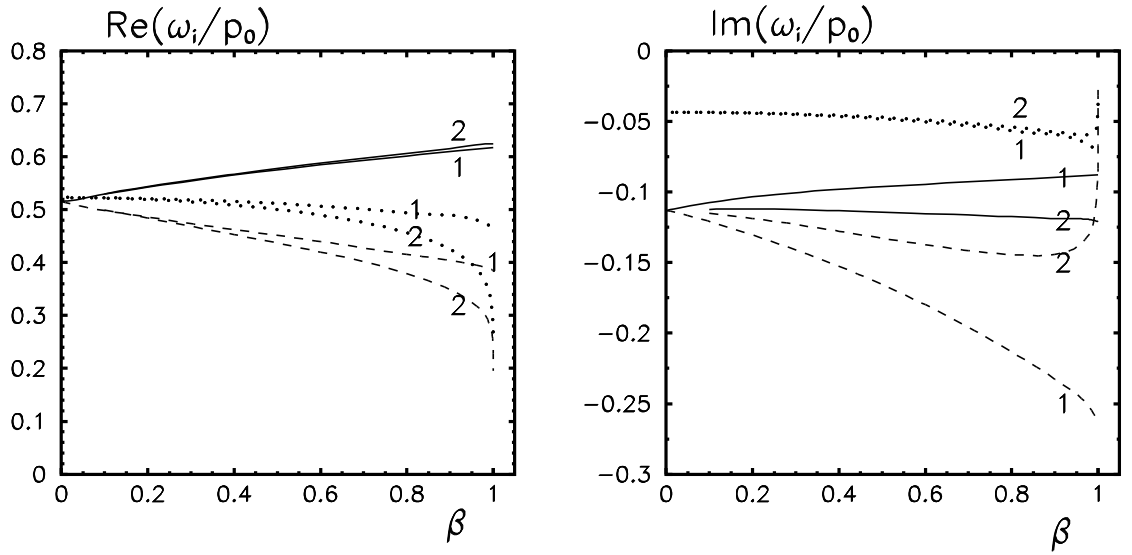


Figure 9: Behavior of  $\omega_{sp}(k, \beta)$ ,  $\omega_{sn}(k, \beta)$  and  $\omega_{snp}(k, \beta)$  at  $\beta \rightarrow 1$ . The wave vector  $k$  is fixed:  $k = p_0$ . Solid curves denote  $\omega_{sn}(k = p_0, \beta)$ , dashed curves –  $\omega_{sp}(k = p_0, \beta)$  and dotted curves are for  $\omega_{snp}(k = p_0, \beta)$ . The number '1' marks solutions of Eq. (11) and '2' - solutions of Eq. (14).



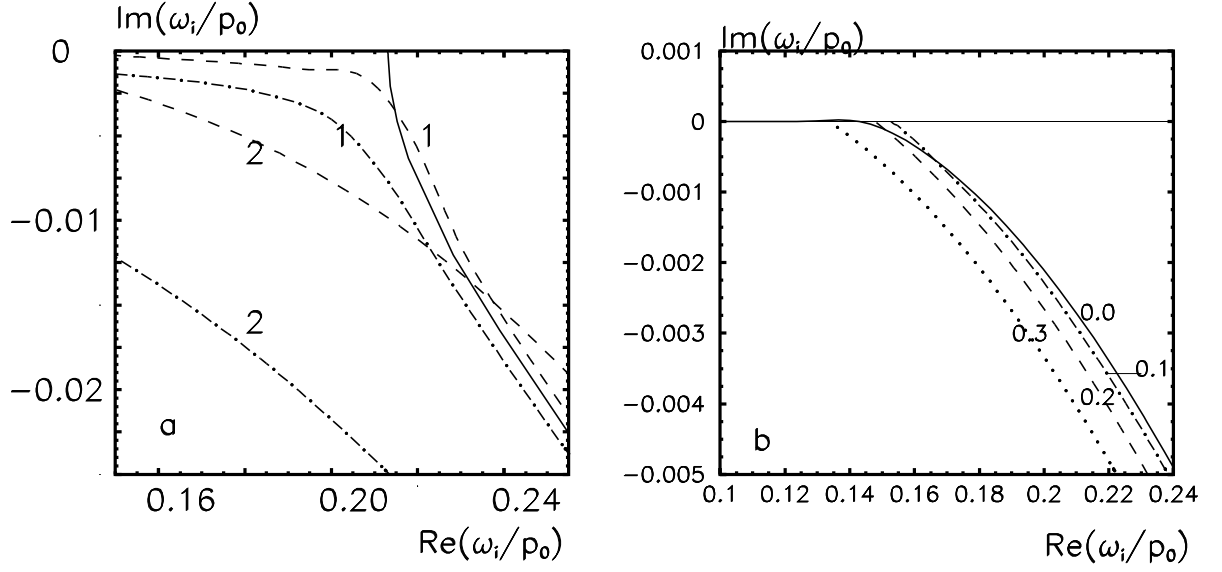


Figure 10: Behavior of  $\omega_{sp}(k, \beta)$ ,  $\omega_{sn}(k, \beta)$  and  $\omega_{snp}(k, \beta)$  at  $\beta \rightarrow 0$ . The complex  $\omega$ -plane. (a): The branches  $\omega_{sn}(k, \beta)$  (dashed-dotted) and  $\omega_{sp}(k, \beta)$  (dashed) for  $\beta=0.01$  (noted by '1') and for  $\beta=0.1$  (noted by '2') in comparison with  $\omega_{s1}(k)$  (solid) calculated for  $\beta=0$ . (b): The branches  $\omega_s(k)$  (solid curve) and  $\omega_{snp}(k, \beta)$  at  $\beta=0.1, 0.2, 0.3$  (the curves dot-dashed, dashed, dotted).

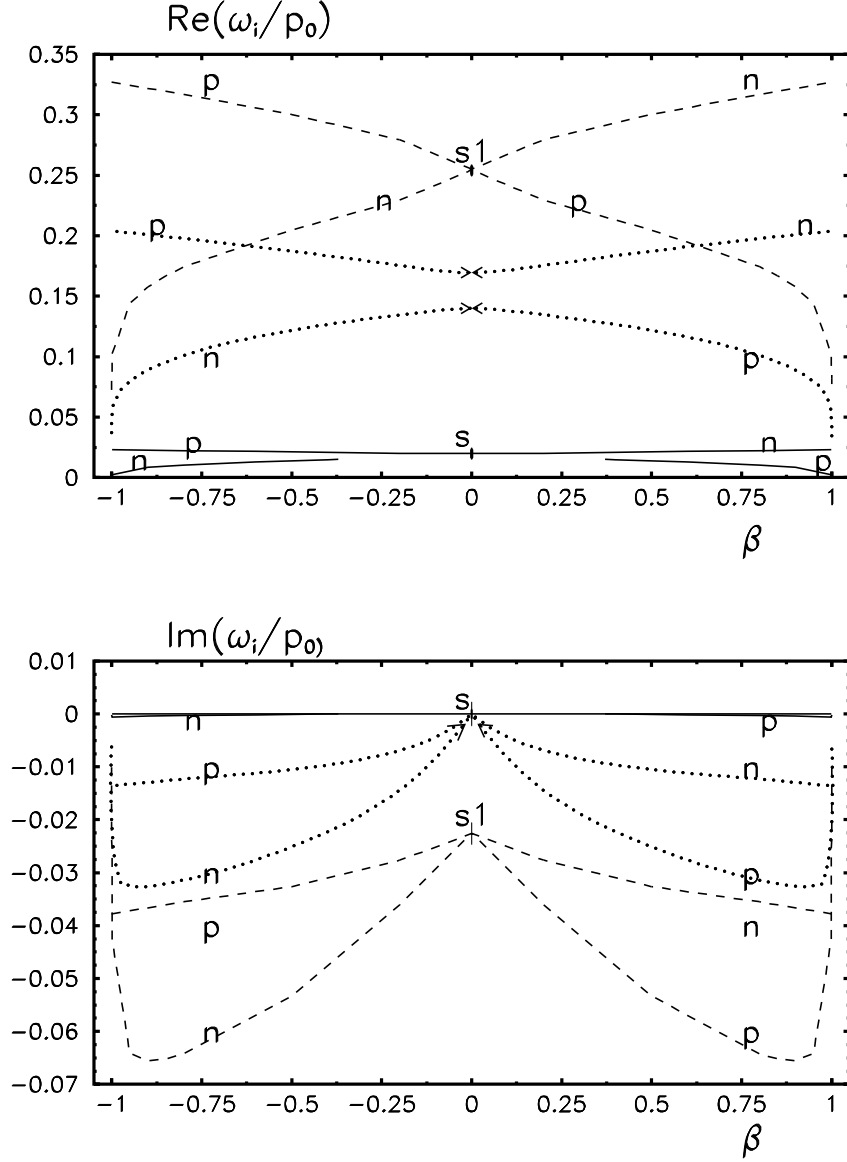


Figure 11: Dependence of the real and imaginary parts of  $\omega_{sn}(k_i, \beta)$  and  $\omega_{sp}(k_i, \beta)$  on  $\beta$  at definite  $k_i$ ,  $i=1,2,3$ . Solid lines  $k_1 = 0.05p_0$ , dotted lines  $k_2 = 0.4p_0$ ; dashed lines  $k_3 = 0.6p_0$ ; 'n' marks  $\omega_{sn}(k_i, \beta)$ , 'p'= $\omega_{sp}(k_i, \beta)$ ; 's'= $\omega_s(k_1)$ , 's1'= $\omega_{s1}(k_3)$ .

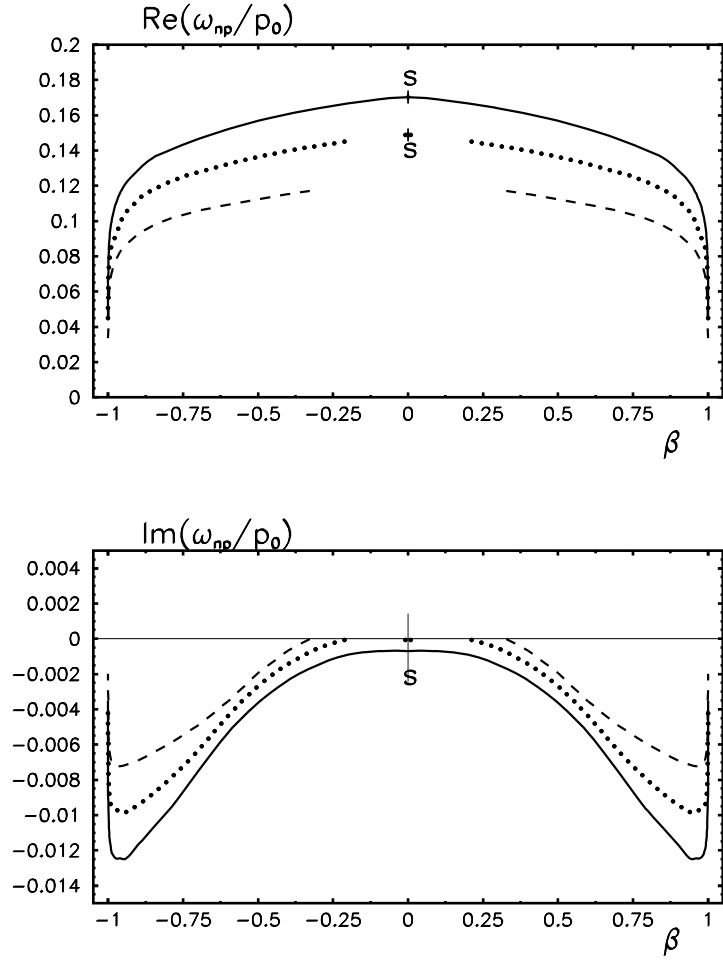


Figure 12: Dependence of the real and imaginary parts of  $\omega_{snp}(k_i, \beta)$  on  $\beta$  at definite  $k_i$ ,  $i=1,2,3$ . Solid lines  $k_3 = 0.4p_0$ , dotted lines  $k_2 = 0.355p_0$ ; dashed lines  $k_1 = 0.3p_0$ ; 's' marks  $\omega_s(k_1)$  and  $\omega_s(k_2)$ .